

THE MUON  $g - 2$  FOR LOW-MASS PSEUDOSCALAR HIGGS IN THE GENERAL 2HDM\*

ADRIANO CHERCHIGLIA

Universidade Federal do ABC, Centro de Ciências Naturais e Humanas  
Santo André, Brazil

DOMINIK STÖCKINGER, HYEJUNG STÖCKINGER-KIM

Institut für Kern- und Teilchenphysik, TU Dresden, 01069 Dresden, Germany

*(Received November 19, 2017)*

The two-Higgs doublet model provides a simple and attractive extension of the Standard Model. It provides a possibility to explain the large deviation between theory and experiment in the muon  $g - 2$  in an interesting parameter region: light pseudoscalar Higgs  $A$ , large Yukawa coupling to  $\tau$ -leptons, and general, non-type II Yukawa couplings are preferred. This parameter region is explored, experimental limits on the relevant Yukawa couplings are obtained, and the maximum possible contributions to the muon  $g - 2$  are discussed.

DOI:10.5506/APhysPolB.48.2147

**1. Introduction**

So far the experiments at the LHC have not identified clear evidence for physics beyond the Standard Model (SM). This is regularly taken as an indication that new physics particles, if they exist, must be rather heavy. The persisting discrepancy between measurement and SM theory in the muon anomalous magnetic moment  $a_\mu$ , however, cannot be explained by arbitrarily heavy new particles. Currently, it is given by

$$a_\mu^{\text{Exp-SM}} = (26.1 \pm 8.0) \times 10^{-10} \quad [1]. \quad (1)$$

This situation has motivated extensive studies of  $a_\mu$  in cases with high-mass new physics. *E.g.* Ref. [2] has studied the largest possible  $a_\mu$  contributions

---

\* Presented at the XLI International Conference of Theoretical Physics “Matter to the Deepest”, Podlesice, Poland, September 3–8, 2017.

in the MSSM and identified the largest possible SUSY mass scale for which the current  $a_\mu$  deviation could be fully explained. Reference [3] considered precision computations in the MSSM, which are particularly important in cases with a partially heavy spectrum of supersymmetric particles, and all these results were implemented in the program GM2Calc [4].

In the remainder of these proceedings, we focus on an alternative idea to consider models which can provide significant contributions to  $a_\mu$  only for very light new particles, which however are nevertheless still viable. Specifically, we focus on the 2-Higgs doublet model (2HDM), the model realizing a non-minimal scalar sector breaking electroweak symmetry in the simplest possible way. It has been known for a long time that it can give rise to significant contributions to  $a_\mu$  only if one of the extra Higgs bosons, specifically the pseudoscalar  $A$ -boson, is fairly light, lighter than the observed SM-like Higgs boson with mass of 125 GeV. Recently, it has been stressed that the parameter space relevant for this is still viable, see particularly Refs. [5, 6].

In Ref. [7], the 2HDM prediction for  $a_\mu$  has been derived at the full two-loop level (which corresponds to leading order), and in a forthcoming reference [8], experimental constraints are exploited to obtain the possible allowed ranges of all contributions and thus identify the parameter space of the general 2HDM, which can explain  $a_\mu$ . Here, we review these results.

## 2. Two-Higgs doublet model

We consider the general 2HDM with only few restrictions on the parameters. We take the Higgs potential to be [9, 10]

$$\begin{aligned} V(\phi_1, \phi_2) = & m_{11}^2 \phi_1^\dagger \phi_1 + m_{22}^2 \phi_2^\dagger \phi_2 - m_{12}^2 (\phi_1^\dagger \phi_2 + \phi_2^\dagger \phi_1) \\ & + \frac{\lambda_1}{2} (\phi_1^\dagger \phi_1)^2 + \frac{\lambda_2}{2} (\phi_2^\dagger \phi_2)^2 + \lambda_3 \phi_1^\dagger \phi_1 \phi_2^\dagger \phi_2 \\ & + \lambda_4 \phi_1^\dagger \phi_2 \phi_2^\dagger \phi_1 + \frac{\lambda_5}{2} \left[ (\phi_1^\dagger \phi_2)^2 + (\phi_2^\dagger \phi_1)^2 \right], \end{aligned} \quad (2)$$

where we only neglect the so-called  $\lambda_{6,7}$  parameters, which we checked to have negligible influence on our later results.

The potential parameters determine the physical masses  $M_{h,H,A,H^\pm}$ , where  $h$  corresponds to the SM-like Higgs boson,  $H$  is assumed to be heavier,  $A$  is a CP-odd scalar, and  $H^\pm$  is a charged Higgs boson. Further, the potential determines the ratio between the two vacuum expectation values,  $\tan \beta$ , and the mixing angle  $\eta \equiv \frac{\pi}{2} - (\beta - \alpha)$ , which LHC-data forces to be small.

The Yukawa couplings are assumed to be “aligned” in the sense of Ref. [11]. *I.e.* we do not assume one of the usual type I, II, X, Y models but only require that the couplings of both Higgs doublets to fermions are proportional to each other, to prevent violations of FCNC bounds. The Yukawa couplings between the scalar  $\mathcal{S}$  and fermion  $f$  are then determined by the factors  $Y_f^{\mathcal{S}}$  given for small  $\eta$  by

$$\begin{aligned} Y_f^h &= 1 + \eta \zeta_f, & Y_f^H &= -\zeta_f + \eta, \\ Y_f^A &= -\Theta_f^A \zeta_f, & \Theta_{d,l}^A &= 1, & \Theta_u^A &= -1. \end{aligned} \quad (3)$$

The units are such that the respective SM-coupling would correspond to  $Y_f^h = 1$ . The couplings depend on the fermion type,  $f \in \{u, d, l\}$ .

In contrast to the usual type I, II, X, Y models, the Yukawa couplings are determined by free parameters  $\zeta_{u,d,l}$  for each fermion type, but they are independent of  $\tan \beta$ .  $\tan \beta$  is a parameter whose role is confined to the Higgs sector.

### 3. Muon $g - 2$ in the 2HDM at two-loop order

In the 2HDM, the muon  $g - 2$  receives contributions from one-loop and two-loop diagrams. The one-loop diagrams, however, are suppressed by two additional powers of the muon mass and thus very small (except at Higgs masses below around 20 GeV). The parametrically leading diagrams are of two-loop order. In this sense, Ref. [7] has completed the full leading-order computation of  $a_\mu$  in the 2HDM; see Ref. [12] for a previous advanced calculation and references to earlier works.

The full result, including one- and two-loop contributions, can be written as

$$a_\mu^{2\text{HDM},2} = a_\mu^{2\text{HDM},1} + a_\mu^{\text{B}} + a_\mu^{\text{F}} + a_\mu^{\Delta r\text{-shift}}. \quad (4)$$

We now briefly discuss all contributions.

- $a_\mu^{2\text{HDM},1}$  are the 2HDM one-loop contributions (which are not contained in the SM prediction). They arise from one-loop diagrams with a single Higgs exchange and are suppressed by two powers of the muon mass divided by the Higgs mass. We will later consider the case of light CP-odd scalar mass  $M_A$ . In this case, the one-loop contributions are negative and make it more difficult to explain deviation (1).
- $a_\mu^{\text{B}}$  are the bosonic two-loop contributions, *i.e.* the contributions arising from diagrams without closed fermion loop. They contain the diagrams with three vertices on the muon line, shown in Fig. 1, and computed for the first time in Ref. [7], but also Barr–Zee-type diagrams with

charged Higgs loop, computed in Ref. [12] and Ref. [7] using different methods. They turn out to be rather small and dominated by diagrams which involve the triple Higgs coupling  $C_{HH^+H^-}$  between  $H$  and two charged Higgs bosons.

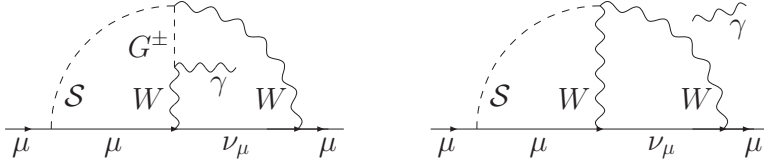


Fig. 1. Bosonic two-loop diagrams with three vertices on the fermion line. From [7].

- $a_\mu^F$  are the two-loop contributions with closed fermion loop. These are dominated by 3<sup>rd</sup>-generation fermions, which have the largest Yukawa couplings. Among the common type I, II, X, Y models, only the type X (or lepton-specific) model is capable of providing significant contributions [5]; in this case, the  $\tau$ -loop contributions are proportional to  $\zeta_l = -\tan\beta$  and dominate by far, but top- and bottom-loop contributions are suppressed as  $1/\tan\beta$ . In the more general aligned model, the top-loop can also contribute significantly (see later and Ref. [6]).
- $a_\mu^{\Delta r\text{-shift}}$  is a shift required because the SM contribution is parametrized in terms of the muon decay constant which receives additional 2HDM contributions. This contribution is below  $2 \times 10^{-12}$  and will hence be neglected in the following.

Useful numerical approximations for the contributions are, using  $\hat{x}_S \equiv M_S/100$  GeV,

$$a_\mu^{2\text{HDM},1} \simeq \left(\frac{\zeta_l}{100}\right)^2 \left[ \frac{3}{\hat{x}_H^2} - \frac{3}{\hat{x}_A^2} - \frac{0.04}{\hat{x}_{H^\pm}^2} \right] \times 10^{-10}, \quad (5)$$

$$a_\mu^B \simeq \frac{\zeta_l}{100} [-4 \dots 4] \times 10^{-10}, \quad (6)$$

$$a_\mu^F \simeq \left[ \left(\frac{\zeta_l}{100}\right)^2 \frac{10}{\hat{x}_A^2} + \frac{-\zeta_l \zeta_u}{100} \frac{20}{\hat{x}_A^2} \right] \times 10^{-10}. \quad (7)$$

The terms in the last line are mainly due to two-loop diagrams with  $\tau$ -loop and top-loop, respectively, and the range given for  $a_\mu^B$  corresponds to varying the Higgs potential parameters in the range allowed by perturbativity.

#### 4. Muon $g - 2$ contributions constrained by experiment

In this section, we provide an overview of the three single largest contributions to  $a_\mu$  in the 2HDM and describe how they are constrained by current experiments.

- $\tau$ -loop contribution: the most important contribution is given by the Barr–Zee-like two-loop diagram with a  $\tau$ -loop generating a  $\gamma\text{--}\gamma\text{--}A$  interaction. The diagram has a behaviour proportional to  $\zeta_l^2/M_A^2$ , see approximation (7). Hence, it is of interest to determine in general the constraints on the lepton Yukawa parameter  $\zeta_l$ .

Such constraints have already been studied in the literature, particularly in Refs. [5, 13], for the type X model, where  $\zeta_l = -\tan\beta$ . The constraints found there arise from  $\tau$ -decays, which can be influenced by additional 2HDM contributions, and by universality of  $Z \rightarrow ll$  decays. Figure 2 (left) shows a scatter plot of allowed parameter points in the 2HDM in the  $M_A\text{--}\zeta_l$  plane, for fixed  $M_H = M_{H^\pm} = 200$  GeV and  $\zeta_u = 0$ , where consistency with  $\tau$ -decays and  $Z \rightarrow ll$  was checked as described in Ref. [13], and consistency with Higgs measurements was checked using 2HDMC and HiggsBounds [14, 15]. The scatter plot shows that the  $\tau$ -decay and  $Z \rightarrow ll$  constraints carry over from

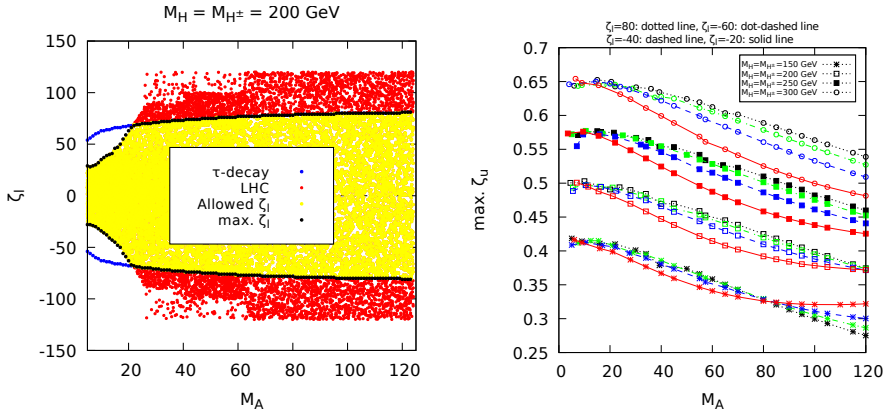


Fig. 2. Left: Scatter plot of the possible parameter points in the 2HDM in the  $M_A\text{--}\zeta_l$  plane, for fixed  $M_H = M_{H^\pm} = 200$  GeV and  $\zeta_u = 0$ . Light grey (yellow) points correspond to the points allowed both by collider constraints (labelled by “LHC”) and  $\tau$ -physics constraints, grey (red) and grey part of line (blue) corresponds to the points allowed by one of these constraints, ignoring the other one. The result for the allowed  $\zeta_l$  values corresponds to the maximum allowed values of  $\tan\beta$  in the 2HDM type X, studied in Ref. [13]. Right: Maximum values of the top-Yukawa parameter  $\zeta_u$  allowed by  $B$ -physics (see the text), as a function of  $M_A$ .

the type X model to the more general model without change, and that there is a small region at very small  $M_A$ , which turns out to be excluded by LEP measurements. We refer to Ref. [8] for further details.

The exclusion bound depends slightly on the chosen values of  $M_H$  and  $M_{H^\pm}$ , but generally the maximum allowed value of  $|\zeta_l|$  varies between around 40 (for smaller Higgs masses) and 100 (for larger Higgs masses).

- Top-loop contribution: the next important contribution is given by the Barr–Zee-like two-loop diagram with a top-loop. It depends on  $\zeta_u \zeta_l / M_A^2$ , and hence the constraints on  $\zeta_u$  are now crucial.

$\zeta_u$  is constrained by  $B$ -physics and by direct Higgs searches. It is clear that these diagrams depend on the same parameters  $\zeta_u, \zeta_l, M_A$  as the desired  $a_\mu$ -contribution. Using the results of Ref. [16], we found that the most constraining  $B$ -physics observables are  $b \rightarrow s\gamma$  and  $B_s \rightarrow \mu\mu$ . Implementing them and checking consistency with data, we obtain the plot of Fig. 2 (right), showing the maximum allowed values of  $\zeta_u$ , as a function of  $M_A$ , for various choices of  $\zeta_l$  and the other Higgs masses. The maximum allowed values are between  $\zeta_u < 0.3$  and  $\zeta_u < 0.7$ .

The constraints from LHC Higgs searches place additional limits on  $\zeta_u$ , which have a more intricate parameter dependence. We provide an example of the LHC constraints for  $M_A = 80$  GeV and  $\zeta_l = -40$  and  $M_H = M_{H^\pm} \in [200, 300]$  GeV in Fig. 3 (left). The colours show parameter points in the  $\zeta_u$ – $C_{HH^+H^-}$  plane which successively fulfil bounds from  $S, T, U$  parameters, HiggsBounds, HiggsSignals, and tree-level stability, unitarity and perturbativity (checked by 2HDMC [15]). The decisive constraints are perturbativity, which provides an upper limit on the triple Higgs coupling  $C_{HH^+H^-}$ , and the LHC constraint on the  $H \rightarrow \tau\tau$  decay. The latter constraint limits  $\zeta_u$  as a function of the triple Higgs coupling, because Higgs production is governed by  $\zeta_u$ , while the branching fraction for the decay to  $\tau\tau$  can be suppressed by large triple Higgs coupling. In the example of Fig. 3 (left), the LHC constraints on  $\zeta_u$  are weaker than the ones from  $B$ -physics. This is true in a significant part of the parameter space, hence we will not discuss these LHC constraints further here and refer to Ref. [8] for details.

- Bosonic contributions: in the promising parameter region with small  $M_A$ , the bosonic contributions are dominated by the Barr–Zee-like diagram with charged Higgs loop and scalar  $H$  exchange. It is proportional to the triple Higgs coupling, which appears in Fig. 3 (left). Inserting the upper limit on the triple Higgs coupling, we obtain the range found in Eq. (6).

$$M_A = 80 \text{ GeV}, M_H = M_{H^\pm} = [200, 300] \text{ GeV}, \zeta_l = -40$$

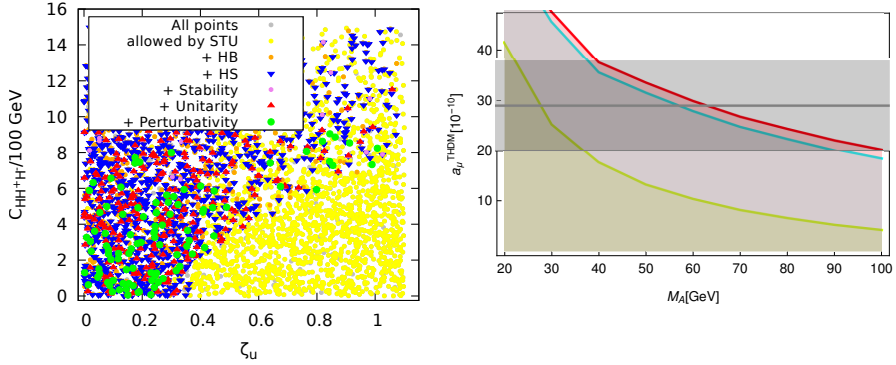


Fig. 3. Left: Allowed ranges of  $\zeta_u$  and the triple Higgs coupling  $C_{HH^+H^-}$ , given certain constraints, see the legend and text. The constraints are applied successively. Right: Approximate maximum values of the two-loop contribution to  $g - 2$  in the general 2HDM for  $M_H = M_{H^\pm} = 200 \text{ GeV}$ , given the constraints discussed in the text. The lowest curve corresponds to the maximum contribution from the  $\tau$ -loop alone, equivalent to the type X model. The middle curve corresponds to adding the maximum possible top-loop contribution, and the top curve to the overall maximum contribution, including bosonic two-loop contributions.

Combining all the results on upper limits on  $\zeta_l$ ,  $\zeta_u$ , and on the bosonic contributions, we can obtain the maximum possible 2HDM two-loop contribution to  $a_\mu$ , as a function of  $M_A$ , for fixed values of the other Higgs masses. Figure 3 (right) shows the resulting maximum contribution for  $M_H = M_{H^\pm} = 200 \text{ GeV}$ <sup>1</sup>. For each  $M_A$ , we first maximize  $\zeta_l$ . This provides the lower curve, which corresponds to the  $\tau$ -loop alone, equivalent to the result in the type X model. Then, for the given  $M_A$  and  $\zeta_l$ , we maximize  $\zeta_u$ , given  $B$ -physics and LHC constraints. This provides the middle curve, corresponding to the maximum full fermionic two-loop contribution in the general 2HDM. Adding the maximum bosonic two-loop contribution then yields the upper curve.

The figure shows that the 2HDM is well capable of providing large contributions to  $a_\mu$ , even larger than deviation (1). However, the necessary parameter region is quite specific: the CP-odd Higgs boson mass must be smaller than  $M_Z$ , and  $\zeta_u$  and  $\zeta_l$  must both be close to their respective maximum values. In particular, going beyond the type X model, *i.e.* having  $\zeta_u$  of the order of 1 instead of the order of  $1/|\zeta_l|$ , increases the maximum  $a_\mu$  almost by a factor two.

<sup>1</sup> This plot is based on approximate results for the experimental constraints; the exact result is very similar and will be presented in Ref. [8].

## REFERENCES

- [1] K. Hagiwara *et al.*, *J. Phys. G* **38**, 085003 (2011) [arXiv:1105.3149 [hep-ph]].
- [2] M. Bach, J.h. Park, D. Stöckinger, H. Stöckinger-Kim, *J. High Energy Phys.* **1510**, 026 (2015) [arXiv:1504.05500 [hep-ph]].
- [3] H.G. Fargnoli *et al.*, *Phys. Lett. B* **726**, 717 (2013) [arXiv:1309.0980 [hep-ph]]; *J. High Energy Phys.* **1402**, 070 (2014) [arXiv:1311.1775 [hep-ph]].
- [4] P. Athron *et al.*, *Eur. Phys. J. C* **76**, 62 (2016) [arXiv:1510.08071 [hep-ph]].
- [5] A. Broggio *et al.*, *J. High Energy Phys.* **1411**, 058 (2014) [arXiv:1409.3199 [hep-ph]].
- [6] T. Han, S.K. Kang, J. Sayre, *J. High Energy Phys.* **1602**, 097 (2016) [arXiv:1511.05162 [hep-ph]].
- [7] A. Cherchiglia, P. Kneschke, D. Stöckinger, H. Stöckinger-Kim, *J. High Energy Phys.* **1701**, 007 (2017) [arXiv:1607.06292 [hep-ph]].
- [8] A. Cherchiglia, D. Stöckinger, H. Stöckinger-Kim, arXiv:1711.11567 [hep-ph].
- [9] G.C. Branco *et al.*, *Phys. Rep.* **516**, 1 (2012) [arXiv:1106.0034 [hep-ph]].
- [10] J.F. Gunion, H.E. Haber, *Phys. Rev. D* **67**, 075019 (2003) [arXiv:hep-ph/0207010].
- [11] A. Pich, P. Tuzon, *Phys. Rev. D* **80**, 091702 (2009) [arXiv:0908.1554 [hep-ph]].
- [12] V. Ilisie, *J. High Energy Phys.* **1504**, 077 (2015) [arXiv:1502.04199 [hep-ph]].
- [13] E.J. Chun, J. Kim, *J. High Energy Phys.* **1607**, 110 (2016) [arXiv:1605.06298 [hep-ph]].
- [14] P. Bechtle *et al.*, *Eur. Phys. J. C* **74**, 2693 (2014) [arXiv:1311.0055 [hep-ph]].
- [15] D. Eriksson, J. Rathsmann, O. Stal, *Comput. Phys. Commun.* **181**, 189 (2010) [arXiv:0902.0851 [hep-ph]]; **181**, 833 (2010).
- [16] T. Enomoto, R. Watanabe, *J. High Energy Phys.* **1605**, 002 (2016) [arXiv:1511.05066 [hep-ph]].